[CANCER RESEARCH 63, 3575–3584, July 1, 2003]

Castration-Induced Increases in Insulin-Like Growth Factor-Binding Protein 2 Promotes Proliferation of Androgen-independent Human Prostate LNCaP Tumors[1]

Satoshi Kiyama, Kevin Morrison, Tobias Zellweger, Majid Akbari, Michael Cox, Duan Yu, Hideaki Miyake, and Martin E. Gleave[2]

The Prostate Centre, Vancouver General Hospital, Vancouver, British Columbia, V6H 3Z6 Canada, and Division of Urology, University of British Columbia, Vancouver, British Columbia, V5Z 3J5 Canada

ABSTRACT

Activation of alternative growth factor pathways after androgen withdrawal is one mechanism mediating androgen-independent (AI) progression in advanced prostate cancer. Insulin-like growth factor (IGF) I activation is modulated by a family of IGF binding proteins (IGFBPs). Although IGFBP-2 is one of the most commonly overexpressed genes in hormone refractory prostate cancer, the functional significance of changes in IGF-I signaling during AI progression remains poorly defined. In this article, we characterize changes in IGFBP-2 in the LNCaP tumor model after androgen withdrawal and evaluate its functional significance in AI progression using gain-of-function and loss-of-function analyses. IGFBP-2 mRNA and protein levels increase 2–3-fold after androgen withdrawal in LNCaP cells *in vitro* in LNCaP tumors during AI progression *in vivo*. Increased IGFBP-2 levels after castration were also identified using a human prostate tissue microarray of untreated and posthormone therapy-treated prostatectomy specimens. LNCaP cell transfectants that stably overexpressed IGFBP-2 progressed more rapidly after castration than control tumors. Antisense oligonucleotides (ASOs) targeting the translation initiation site of IGFBP-2 reduced IGFBP-2 mRNA and protein expression by >70% in a dose-dependent and sequence-specific manner. ASO-induced decreases in IGFBP-2-reduced LNCaP cell growth rates and increased apoptosis 3-fold. LNCaP tumor growth and serum prostate-specific antigen levels in mice treated with castration plus adjuvant IGFBP-2 ASOs were significantly reduced compared with mismatch control oligonucleotides. Increased IGFBP-2 levels after androgen ablation may represent an adaptive response that helps potentiate IGF-I-mediated survival and mitogenesis and promote androgen-independent tumor growth. Inhibiting IGFBP-2 expression using ASO technology may offer a treatment strategy to delay AI progression.

INTRODUCTION

Prostate cancer is the most common cancer that affects men and the second leading cause of cancer deaths in men in the Western world. Because prostate cancer is an androgen-sensitive tumor, androgen withdrawal, for example, via castration, is used in some therapeutic regimens for patients with advanced prostate cancer. Androgen withdrawal is the only effective form of systemic therapy for men with advanced disease, producing symptomatic and/or objective response in 80% of patients. Unfortunately, AI[3] progression and death occurs within a few years in the majority of these cases (1). HRPC is highly chemoresistant with objective response rates of 10% and no demonstrated survival benefit (2). More recently, Phase II studies using taxane-based combination regimens are reporting objective responses in 20–30% and PSA responses in >50% of cases (3–5). HRPC remains the main obstacle to improving the survival and quality of life in patients with advanced disease. Novel therapeutic strategies that target the molecular basis of androgen and chemoresistance may provide an opportunity to delay progression and prolong survival.

One mechanism mediating AI progression in advanced prostate cancer involves activation of alternative growth factor pathways after androgen withdrawal. The IGF system, which consists of two ligands, IGF-I and IGF-II, plays an important role in cell growth regulation, transformation, and tumorigenesis (6, 7). The mitogenic and antiapoptotic activity of IGF is modulated by six IGFBPs (7–10). These IGFBPs are synthesized locally in most tissues, including cancer cells, to inhibit or enhance IGF actions and may even possess ligand-independent activity (11–13). During tissue development, IGFBPs are expressed in a tissue- and stage-specific manner (14, 15).

Among the IGFBPs, IGFBP-2 has been shown to function as an enhancer of IGF-I function in several cell lines (16–18). Although IGFBP-2 is normally expressed in fetal cells and low or absent in many adult tissues, high levels of IGFBP-2 are associated with carcinogenesis or tumor progression in several tumor tissues. Elevated serum levels of IGFBP-2 have been reported in ovarian (19), colon (20), central nervous system (21), and prostate (22–24) cancers. IGFBP-2 immunohistochemical staining levels are higher in high Gleason grade cancers compared with low-grade cancers or benign epithelial cells (25) and in recurrent AI tumors compared with untreated hormone naïve tumors (26). Experimentally, IGFBP-2 expression levels also increase after castration in the rat ventral prostate (27) and during AI progression in AD Shionogi (28) and CRW22 (29) prostate cancer models and in human prostate tumors (25, 30, 31). Additionally, long-term overexpression of IGFBP-2 in adenocortical tumor cells enhanced cell proliferation and increased cloning efficiency (18). Transfection of IGFBP-2 to human epidermoid carcinoma increases tumorigenesis (32). Collectively, these observations suggest that changes in IGF/IGFBP-2 signaling may represent activation of an alternative growth factor pathway involved in AI progression.

Elucidation of the pathogenic role of candidate genes implicated in tumor progression is a rapidly progressing field of cancer research and has provided a steadily growing list of candidates. Known nucleotide sequences of cancer-relevant genes offer the possibility to design tailored anticancer agents that lack many of the toxic side effects displayed by conventional therapeutics. The objective of this study was to define changes in IGFBP-2 expression after castration and during AI progression in the LNCaP tumor model and to evaluate the functional relevance of these changes in AI progression using gain-of-function and loss-of-function analyses. As part of our ongoing investigations to identify important pathways mediating AI progression, we have used ASOs to evaluate the functional role of castration-induced changes in Bcl-2 (33), Bcl-xL (34), clusterin (35), and

Received 7/16/02; accepted 4/29/03.

The costs of publication of this article were defrayed in part by the payment of page charges. This article must therefore be hereby marked *advertisement* in accordance with 18 U.S.C. Section 1734 solely to indicate this fact.

[1] This work was supported by Grant 009002 from the National Cancer Institute of Canada and the Hudson Fund at the Vancouver General Hospital.

[2] To whom requests for reprints should be addressed, at Division of Urology, University of British Columbia, D-9, 2733 Heather Street, Vancouver, British Columbia, V5Z 3J5 Canada.

[3] The abbreviations used are: AI, androgen independent; AD, androgen dependent; ASO, antisense oligonucleotide; HRPC, hormone refractory prostate cancer; IGF, insulin-like growth factor; IGFBP, IGF binding protein; IGF-IR, IGF-I receptor; PSA, prostate-specific antigen; NHT, neoadjuvant hormone therapy; DHT, dihydrotestosterone; G3PDH, glyceraldehyde-3-phosphate dehydrogenase.

IGFBP-5 (36) in prostate xenograft models, some of which are now being evaluated in clinical trials (37, 38). Phosphorothioate ASO are chemically modified stretches of single-stranded DNA complementary to mRNA regions of a target gene, thereby inhibiting gene expression and providing a useful tool for *in vitro* and *in vivo* functional genomics (39–42). For this study, overexpressing IGFBP-2 LNCaP cell transfectants were created to determine whether this changed tumor growth rates and time to AI, whereas IGFBP-2 ASOs were used to determine their effects on IGFBP-2 levels and cell proliferation in LNCaP cells *in vitro* and AI LNCaP tumor growth and PSA levels after castration.

MATERIALS AND METHODS

LNCaP Tumor Growth. The human prostatic carcinoma cell line LNCaP was kindly provided by Dr. Leland W. K. Chung (Emery University, Atlanta, GA) and used in this study. Cells were cultured and maintained in RPMI medium (Life Technologies, Inc.) supplemented with 5% heat-inactivated FCS as described previously (43, 44). For *in vivo* study, $\sim 1 \times 10^6$ LNCaP cells were inoculated s.c. with 0.1 ml of Matrigel (Becton Dickinson Labware, Franklin Lakes, NJ) in the flank region of 6–8 week-old male athymic nude mice (Harlan Sprague Dawley, Inc., Indianapolis, IN) via a 27-gauge needle under methoxyfluorane anesthesia.

Human Prostate Tissue Microarray Preparation. Archival formalin-fixed, paraffin-embedded human prostate tumor specimens were used to construct a human prostate cancer tissue array of hormone naïve and NHT-treated samples. A total of 190 specimens was obtained from hormone naïve benign ($n = 4$), hormone naïve cancer ($n = 21$), AI ($n = 24$), and after treatment with NHT for 1 month ($n = 56$), 3 months ($n = 24$), and 6–8 months ($n = 56$). The benign samples were obtained from transition zone biopsies of radical prostatectomy specimens, whereas the AI specimens were obtained from transurethral resections of patients with HRPC. Two samples/tumor specimen were arrayed for a total of 380 cores/array. Core tissue biopsy specimens (diameter, 0.6 mm) were taken from preselected regions of individual paraffin-embedded donor blocks and precisely arrayed into a new recipient paraffin block with a tissue arrayer (Beecher Instrument, Silver Spring, MD). After the block construction was completed, 5-μm sections were cut with a microtome by use of an adhesive-coated tape sectioning system (Instrumedics, Hackensack, NJ) to support the adhesion of the array elements.

Mounted tissues on the slides were rehydrated, and endogenous peroxidase activity was blocked with methanol containing H_2O_2. Antigen retrieval was enhanced using Dako Target Retrieval Solution (Dako Corporation, Carpinteria, CA) with the autoclave method. BSA (Promega, Madison, WI) was applied for 1 h at room temperature to block the nonspecific binding sites on the slides, which were then incubated in a humidified chamber overnight at 4°C with a 1:50 dilution (200 μg/ml) of a rabbit antihuman IGFBP-2 polyclonal IgG antibody (Upstate Biotechnology). After primary incubation, tissue was washed three times with PBS and incubated with a horseradish peroxidase-conjugated goat antirabbit IgG secondary antibody (Upstate Biotechnology) used at a 1:400 dilution for 30 min at 25°C. The antigen was visualized by subsequent 5-min incubation with diaminobenzidine tetrahydrochloride before counterstaining with hematoxylin. Tissues were covered with mounting media (Permount; Fisher Scientific, Fair Lawn, NJ) and a coverslip. Negative control slide was processed in an identical fashion to that above, with the substitution of normal goat nonimmune serum for the primary antiserum. No color reactions were observed in negative control slide. Photomicrographs were taken through a microscope coupled to a digital camera, Photometrics CoolSNAP (Roper Scientific, Inc., Glenwood, IL), and corresponding imaging software.

Scoring of IGFBP-2 Staining. The staining intensity of cytoplasmic IGFBP-2 was evaluated and scored by a pathologist (M. A.) and the Image Plus software (Media Cybernetics). Specimens were graded from 0 to +4 intensity, representing the range from no staining to heavy staining. All comparisons of staining intensity and percentages were made at ×400 magnification. Image Pro Plus software quantifies the percentage of stained area (combination of intensity and surface area).

Lentiviral Infection of IGFBP-2 into LNCaP. The full-length cDNA for human IGFBP-2 was a generous gift of Dr. Anand Swaroop (University of Michigan). The 1.4-kb IGFBP-2 cDNA was subcloned into the lentiviral vector pHR′-CMV-EGFP at the *Bam*HI and *Xho*I sites. Two vectors were created for study: pHR′-CMV-IGFBP-2 and pHR′-CMV (empty vector). Clone identity was verified using restriction digest analysis and plasmid DNA sequencing. Infectious lentivirus was generated by cotransfection of 1.5×10^6 293T cells with target plasmids with pCMVΔR8.2 (carries sequence necessary for viral assembly of lentivirus) and pMD.G, which expresses the vesicular stomatitis virus envelop glycoprotein G(VSV-G) pseudotype as described previously (45). The 293T cells were transfected with either IGFBP-2-expressing, EGFP-expressing, or empty lentiviral vector (10 μg of each) using the calcium phosphate precipitation method (Promega Profection Mammalian Transfection Systems). The 293T cells were transfected for 12–15 h, after which fresh media were added for 24 h. After this, the virus containing media was collected and filtered through 0.45-μm filter. Early-passage LNCaP cells (passage 30) were plated in 10-cm plates, and competent retrovirus was added to 30–40 multiplicity of infection. The media were changed after incubation for 16 h. The cells were passaged and harvested for UV microscopy to verify green fluorescent protein expression. Total RNA, conditioned media, and whole cell lysate were collected to ensure expression of IGFBP-2 by Western blotting and real-time PCR.

Antisense IGFBP-2 Oligonucleotides. Phosphorothioate oligonucleotides used in this study were generated by Operon (Alameda, CA). Three different sequences of IGFBP-2 ASOs were designed. One was designed to hybridize with the translation initiation site (5′-GCAGCCCACTCTCGGCAGCAT-3′), with two others designed randomly (5′-CGCCCAGTAGCAGCAGCAGCA-3′ and 5′-TCCCGGAACACGGCCAGCTCC-3′). Two-base IGFBP-2 mismatch oligonucleotides (5′-GCAGCCCACTGTCCGCAGCAT-3′, 5′-CGCGCACTAGCAGCAGCAGCA-3′, and 5′-TCCCGGAACTGCCCCAGCTCC-3′, respectively) were also synthesized and used as controls. Oligonucleotides were stored at −20°C in 10 mM Tris and 1 mM EDTA.

Treatment of Cells with Oligonucleotides. Lipofectin, a cationic lipid (Life Technologies, Inc., Gaithersburg, MD), was used to increase uptake of oligonucleotides into cells. LNCaP cells were treated with various concentrations of oligonucleotides by adding 4 mg/ml lipofectin after preincubation for 20 min in serum-free RPMI. Four h after the beginning of the incubation, steroid hormone-depleted, charcoal-stripped media with or without 1 nM DHT (Sigma, St. Louis, MO) were added to the medium, as described previously (36). A second cycle treatment was applied 24 h later.

Northern Blotting Analysis. Total RNA was extracted from cultured LNCaP cells or LNCaP tumors using the acid-guanidinium thiocyanate-phenol chloroform method. A total of 20 μg of RNA from each sample was subjected to electrophoresis on 1.2% agarose-formaldehyde gels and transferred to nylon membranes overnight according to standard procedures (35). Human IGFBP-2 and G3PDH probes were generated by reverse-transcription PCR from RNA of LNCaP cells with using primers 5′-ACAATGGCGATGACCACTCAGA-3′ (sense) and 5′-ACAGCACCATGAACATGTTTG-3′ (antisense) for IGFBP-2 and 5′-TGCTTTTAACTCTGGTAAAGT-3′ (sense) and 5′-ATATTTG-GCAGGTTTTTCTAGA-3′ (antisense) for G3PDH. The RNA blots were hybridized with human IGFBP-2 probe labeled with [^{32}P]dCTP by random primer labeling. Washing and densitometric analysis were carried out as reported previously (36–38). After detecting the IGFBP-2 expression, the membranes were reprobed and rehybridized with human G3PDH probe to verify the integrity of the RNA.

Western Blotting Analysis. Samples containing equal amounts of protein (20 μg) from lysates of the cultured cells were subjected to SDS-PAGE and transferred to nitrocellulose filters. The filters were blocked in PBS containing 7% nonfat skim milk powder at 4°C overnight and then incubated for 1 h with 1:400-diluted anti-IGFPB-2 rabbit polyclonal antiserum (Upstate Biotechnology, Lake Placid, NY) and 1:400-diluted β-actin (Sigma). The filters were then incubated for 30 min with 1:10,000-diluted horseradish peroxidase-conjugated antirabbit or antimouse IgG antibody (Amersham Life Science, Arlington Heights, IL), and specific proteins were detected using an enhanced chemiluminescence Western blotting analysis system (Amersham Life Science).

***In Vitro* Mitogenic Assay.** The *in vitro* growth of LNCaP was assessed by the *in vitro* mitogenic assay, as described previously (43). When LNCaP cells in 10-cm dishes reached 70% confluence, medium was changed to serum-free media for serum starvation. After 24 h of serum starvation, cells were treated with IGFBP-2 ASO or mismatch control with or without DHT, as described above. After treatment, LNCaP cells were fixed with 1% glutaraldehyde (Sigma), stained with 0.5% crystal violet (Sigma), followed by incubation for

4 h at 37°C, and eluted with 10 ml of Sorensen's solution (9 mg of trisodium citrate in 305 ml of distilled water, 195 ml of 0.1 N HCl, and 500 ml of 95% ethanol). The absorbance was determined with a microculture plate reader (Becton Dickinson Labware) at 550 nm. Absorbance values were normalized to the values obtained for the vehicle-treated cells to determine percent survival. Each assay was performed in triplicate.

Flow Cytometric Analysis. Flow cytometric analysis of propidium iodide-stained nuclei was performed as described previously (36). Briefly, the LNCaP cell sublines were plated in 10-cm dishes and, when 70% confluent, were treated as described above. The cells were trypsinized, washed twice with PBS, and fixed in 70% ethanol for 5 h at 4°C. The fixed cells were washed twice with PBS, incubated with 1 μg/ml RNase A (Sigma) for 1 h at 37°C, and stained with 5 μg/ml propidium iodide (Sigma) for 1 h at room temperature. The stained cells were analyzed for relative DNA content on a dual laser flow cytometer (Beckman Coulter epics elite; Beckman, Inc., Miami, FL).

Treatment of Mice with Oligonucleotides *in Vivo*. Mice bearing tumors between 300 and 500 mm^3 in volume were castrated via a scrotal approach and randomly assigned to treatment with 10 mg/kg of either antisense or mismatch IGFBP-2 oligonucleotides i.p. once daily. Treatment commenced beginning 1 day after castration. Tumor volume and serum PSA measurements were performed once weekly. Tumor volumes were calculated by the formula $L \times W \times H \times 0.5236$ (43). Blood samples were obtained from tail vein incisions of mice, and serum PSA levels were determined by an enzymatic immunoassay kit with a lower limit of sensitivity of 0.2 μg/liter (Abbott IMX, Montreal, Quebec, Canada), according to the manufacturer's protocol. Selected tumors were excised for Northern analysis of IGFBP-2 mRNA levels. Data points were expressed as average tumor volumes and serum PSA levels $\pm$ SE. All animal procedures were performed according to the guidelines of the Canadian Council on Animal Care and with appropriate institutional certification.

Statistical Analysis. All data were analyzed by student's *t* test. Levels of statistical significance were set at $P < 0.05$ (two-sided), and all statistical calculations were done by use of the Statview 4.5 (Abacus Concepts, Inc., Berkeley, CA).

RESULTS

Changes in IGFBP-2 Expression after Androgen Withdrawal. We first examined the protein expression pattern of IGFBP-2 in the LNCaP cells cultured in charcoal-stripped serum with or without added androgens (R1881). We found that, over time, there was a relative increase in the protein expression of IGFBP-2 in the cells cultured in conditions that lacked androgens (Fig. 1). Increases in IGFBP-2 levels were also seen under conditions using serum-free media (data not shown).

Northern blotting was used to characterize changes in IGFBP-2 mRNA expression in AD intact tumors before castration and at various time points after castration. As shown in Fig. 2, IGFBP-2 expression increased gradually beginning 14 days after castration and, by 28 days after castration, was >2-fold compared with levels before castration (two-sided $P < 0.05$, student's *t* test).

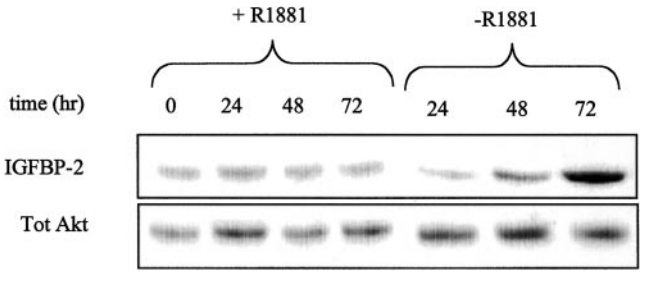

Fig. 1. IGFBP-2 protein levels increase after androgen withdrawal *in vitro*. LNCaP cells were cultured in phenol-red RPMI media containing 5% FBS. At time zero, the cells were passaged into RPMI media with 5% charcoal-stripped serum with or without 0.1 nM R1881 synthetic androgen. Proteins were harvested for Western blotting at specific time intervals. Total protein was quantified using the Bradford assay, and 15 μg of each protein sample were loaded. IGFBP-2 was detected with the Upstate polyclonal antibody, and equal loading was determined by probing for total levels of Akt.

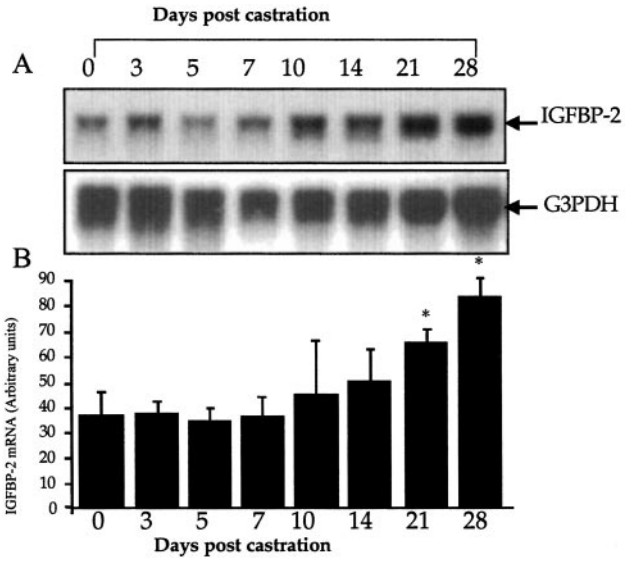

Fig. 2. Castration-induced changes of IGFBP-2 mRNA expression *in vivo*. LNCaP tumors were harvested from intact male athymic mice before and at the indicated time points after castration. *A*, total RNA was extracted from each tumor tissue and analyzed for IGFBP-2 and G3PDH levels by Northern blotting. *B*, quantitative analysis of IGFBP-2 mRNA levels after normalization to G3PDH mRNA levels in LNCaP tumors before and after castration was performed using the laser densitometer. This analysis was repeated three times using three different groups of samples, and each column represents the mean value with SD of Northern blots from three different tumor series. *, significantly different compared with before castration ($P < 0.05$).

Increased IGFBP-2 levels after castration was also identified using a human prostate tissue microarray (Fig. 3). IGFBP-2 staining was absent in benign prostate epithelium (Fig. 3*A*), whereas mean intensity increased from 0.73 in hormone naïve cancers (Fig. 3*B*) to 1.1 after 1 month NHT (Fig. 3*C*), 1.7 after 3 months (Fig. 3*D*), 1.9 after 8 months (Fig. 3*E*), and 2.1 in AI tumors (Fig. 3*F*). Differences in staining between benign and cancer and between hormone naïve and AI tumors were statistically significant (two-sided $P < 0.05$, student's *t* test). Temporal changes in immunostaining in the human prostate tissue microarray corresponded with results from Northern blotting of LNCaP xenografts.

IGFBP-2 Overexpression Promotes AI Tumor Growth *in Vivo*. To characterize the role of IGFBP-2 in AI progression, we generated a cell line that overexpressed IGFBP-2. Using the lentiviral transfection system, we generated a population of LNCaP cells that stably expressed either human IGFBP-2 cDNA (labeled LNBP-2) or an empty lentiviral construct (labeled LNCaP). We verified elevated expression of IGFBP-2 protein in both whole cell lysates and in conditioned media (Fig. 4). Quantitative expression of IGFBP-2 transcripts in the resultant cell lines was determined by real-time PCR and revealed a 100-fold greater expression of IGFBP-2 in the transfected cells (data not shown). We compared the rate of progression to AI in the LNCaP tumor model after castration (defined by a rising PSA after castration) in LNBP-2- and control-transfected LNCaP cells and followed tumor volumes and PSA levels before castration. At a PSA of 75 ng/liter, the mice were castrated, and tumor volumes and PSA measurements were done on a weekly basis. We found that by 2 weeks after castration, the LNBP-2 tumors demonstrated a rapid recovery in tumor growth and rise in PSA consistent with more rapid AI tumor growth compared with mock transfected controls (statistically significant using student *t* test $P < 0.05$, Fig. 5).

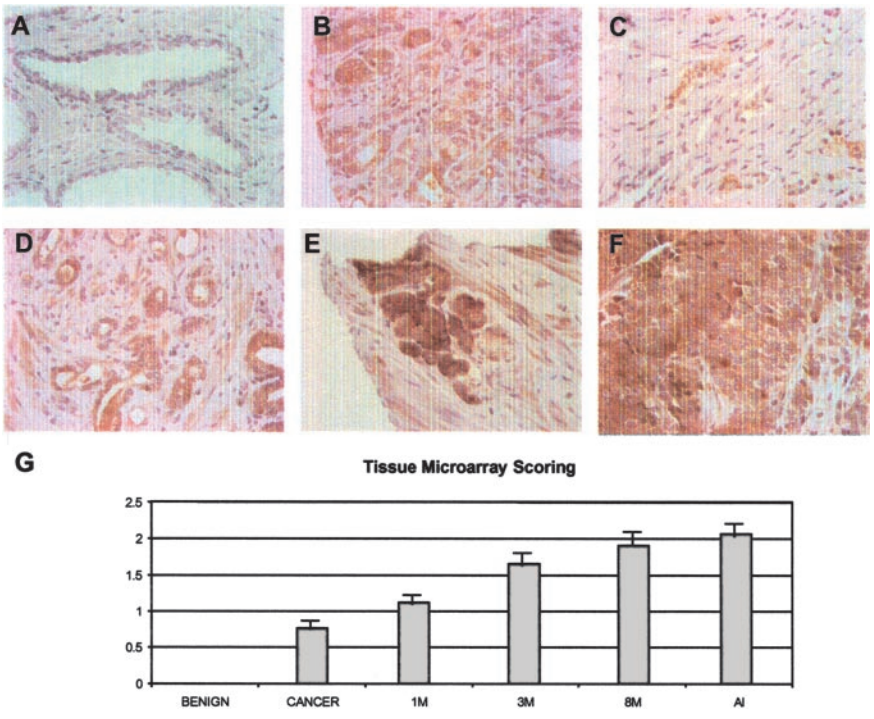

Fig. 3. Immunohistochemical analysis of IGFBP-2 protein using human prostate tissue microarray. Human prostate specimens from benign, untreated cancer, and posthormone therapy cancers were used to construct a tissue microarray and then stained with IGFBP-2 antibody. Representative array cores from benign (*A*), hormone naïve (*B*), and various times after androgen ablation, including 1 month (*C*), 3 months (*D*), 8 months (*E*), and AI tumors (*F*). Mean intensity (±SE) of staining score was significantly higher between benign epithelial and cancer cells (two-sided $P < 0.05$, student's *t* test) and between hormone naïve and >3 months of hormone therapy (*G*; two-sided $P < 0.05$, student's *t* test). Magnification, ×400.

Suppression of IGFBP-2 mRNA and Protein Levels by IGFBP-2 ASO in LNCaP Cells *in Vitro*. The data presented above suggests that increased IGFBP-2 after castration may help accelerate time to AI progression. We next set out to test whether inhibiting IGFBP-2 could inhibit IGF-I signaling and delay time to AI progression. To identify the most effective IGFBP-2 ASO, three different IGFBP-2 ASOs were synthesized and tested for their ability to decrease IGFBP-2 mRNA levels in LNCaP cells. IGFBP-2 mRNA expression was suppressed most effectively by 1000 nM of the ASO targeting the translation initiation site of IGFBP-2 (data not shown). This ASO sequence (5′-GCAGCCCACTCTCGGCAGCAT-3′), along with its 2-base mismatch control (5′-GCAGCCCACTGTCCGCAGCAT-3′) was chosen for subsequent *in vitro* and *in vivo* experiments.

Northern blotting was used to measure changes in IGFBP-2 mRNA expression in LNCaP cells after treatment with IGFBP-2 ASO and mismatch control oligonucleotide. Four days after treatment, IGFBP-2 ASO suppressed mRNA by >70% in a dose-dependent and sequence-specific manner (Fig. 6*A*). These results were confirmed using real-time PCR (data not shown). Similarly, Western blotting analysis was used to show that the observed decrease in IGFBP-2 mRNA levels was paralleled by dose-dependent and sequence-specific decreases in IGFBP-2 protein levels (Fig. 6*B*).

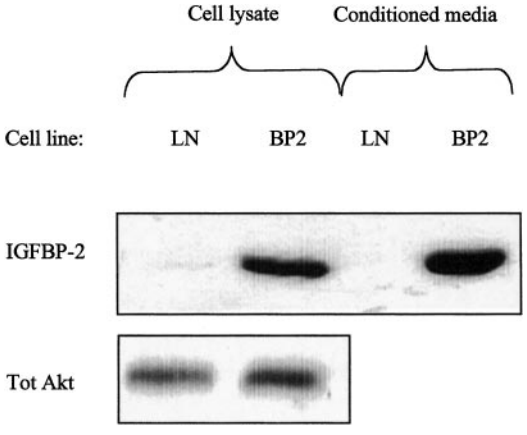

Fig. 4. LNCaP cells infected with IGFBP-2 containing lentivirus express and secrete high levels of IGFBP-2. LNCaP cells infected with vector control lentivirus and lentivirus containing the full-length IGFBP-2 human cDNA were cultured in 5% FBS and then harvested for Western blotting. Conditioned media was collected from both cells lines after incubation in serum-free media for 48 h. The volume of conditioned media from each cell line was normalized to the number of cells/plate/volume of media.

Effects of IGFBP-2 ASO on LNCaP Cell Growth *in Vitro*. To determine whether reduced IGFBP-2 levels alter LNCaP cell growth rates, a mitogenic assay was performed after treatment with IGFBP-2 ASO or mismatch control oligonucleotide in cells cultured in serum-containing media. As shown in Fig. 7, after treatment with 500 nM IGFBP-2 ASO, LNCaP cell numbers decreased in a dose-dependent manner by up to 80% compared with the untreated or mismatch control-treated groups.

To investigate whether androgens altered IGFBP-2 ASO-induced LNCaP cell growth inhibition, LNCaP cells were treated with 500 nM IGFBP-2 ASO with or without 1 nM DHT for 2 days under serum-free conditions (Fig. 8). IGFBP-2 ASO reduced LNCaP cell number by 56% with DHT ($P < 0.05$) and 40% without DHT ($P < 0.05$), compared with the no treated or mismatch control oligonucleotide-treated groups, respectively. Addition of IGF-I with IGFBP-2 ASO blunted the inhibitory effects of IGFBP-2 ASO only when DHT was present, whereas recombinant IGF-I had no effect on LNCaP cell growth in the absence of DHT regardless of IGFBP-2 ASO treatment.

Changes in Cell Cycle Distribution after Treatment with IGFBP-2 ASO. To additionally investigate the effects of IGFBP-2 ASO on LNCaP cell growth, flow cytometric assay was performed. LNCaP cells were treated with IGFBP-2 ASO with or without 1 nM DHT for 2 days. As shown in Fig. 9, IGFBP-2 ASO significantly increased the sub-G_1-G_0 proportion 3-fold ($P < 0.05$) and decreased the S + G_2-M proportion by 50% compared with untreated or mismatch control oligonucleotide-treated cells. The addition of DHT did not significantly alter the effects of IGFBP-2 ASO on cell cycle distribution of sub-G_1-G_0 proportion.

Effects of IGFBP-2 ASO on AI LNCaP Tumor Growth *in Vivo*. To evaluate the efficacy of IGFBP-2 ASO *in vivo*, nude mice bearing LNCaP tumors were castrated and treated with adjuvant IGFBP-2

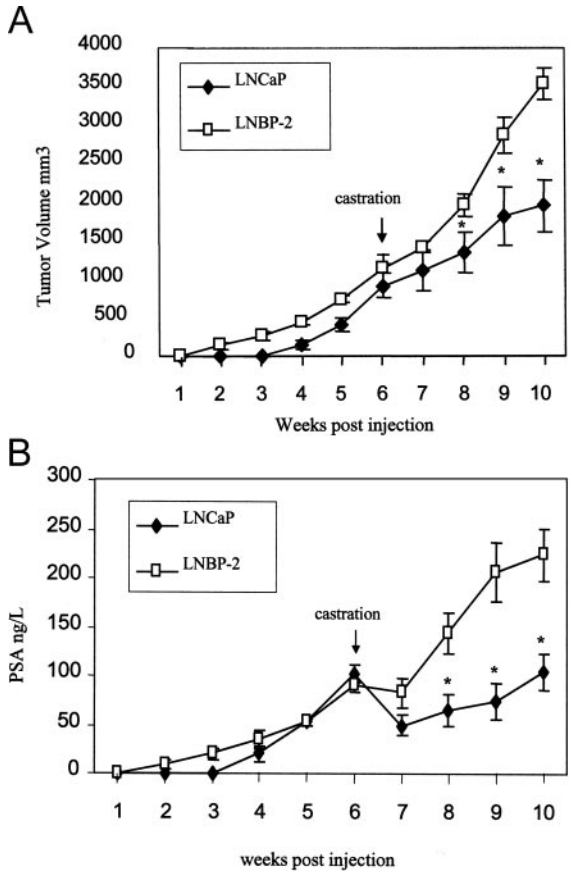

Fig. 5. *A*, LNBP-2 and LNCaP tumor volume in nude mice pre- and postcastration. Ten nude mice were injected with LNBP-2 and LNCaP cells (1×10^6 cells). Tumor volume and serum PSA were monitored weekly once tumors were palpable. The mice were castrated at a PSA threshold of 75 ng/liter. The tumor volumes were monitored pre- and postcastration, and the mean LNBP-2 tumor volume was found to be significantly greater than the LNCaP tumor volume at 3 weeks after castration as indicated by the ∗ symbol. *B*, mean serum PSA in LNBP-2 and LNCaP tumors pre- and postcastration. PSA was measured at weekly intervals. The mice were castrated at a PSA level of ~75 ng/ml. The mean PSA value for the LNBP-2 group became significantly greater than the LNCaP group at 3 weeks after castration, indicating a more rapid time to AI.

ASO or mismatch control oligonucleotide ($n = 7$ in each group). Phosphorothioate oligonucleotides were administered once daily by i.p. injection for 8 weeks. Tumor volume and serum PSA levels were similar before treatment both groups. After castration, mean tumor volume increased more rapidly in the mismatch control oligonucleotide-treated group compared with IGFBP-2 ASO-treated group. By 8 weeks after castration, mean tumor volume in mismatch control treated mice was 1.6-fold higher than the IGFBP-2 ASO-treated group ($P < 0.05$; Fig. 10*A*). After castration, serum PSA levels decreased 60% in both groups but increased more rapidly in the mismatch control oligonucleotide-treated group. By 8 weeks after castration, mean serum PSA level in IGFBP-2 ASO-treated mice was significantly lower than in control mice (211.7 *versus* 388.5 ng/ml, $P < 0.005$; Fig. 10*B*). No significant toxicity or side effects were observed in either group. When LNCaP tumors were harvested for Northern blotting for IGFBP-2, IGFBP-2 mRNA expression in IGFBP-2 ASO-treated groups was significantly lower than mismatch control oligonucleotide-treated groups (after normalization with G3PDH, $P < 0.05$; Fig. 10*C*).

DISCUSSION

The sensitivity of tumor cells to undergo apoptosis in response to cytotoxic stress and their ability to adaptively alter gene expression determines their susceptibility to therapies and survive under adverse physiological conditions. Androgen ablation causes apoptotic prostate cancer cell death, but despite high initial response rates, remissions are temporary because surviving tumor cells eventually recur. Cellular and molecular events that mediate AI progression consist of a complex process involving both clonal selection and adaptive mechanisms occurring in heterogeneous tumors composed of subpopulations of cells that respond differently to androgen withdrawal. Changes in expression of various apoptosis-associated genes, including bcl-2 (33) and clusterin (34), or recruitment of alternative autocrine, paracrine, or endocrine stimulatory pathways that replace androgen requirement for growth and survival (36, 46) are key elements of AI progression.

IGF-I is a potent mitogenic and antiapoptotic factor for various types of normal and malignant tissues, including prostate. Although circulating levels of IGF-I principally arise from the liver, the biological response of cells to IGFs is regulated by several factors in the microenvironment, including the IGFBPs (7–10). To date, at least six IGFBPs have been identified that modulate the biological action of the IGF through high affinity binding interactions that influence the ability of IGF-I to function as ligands for the type I IGF receptor. IGFBP physiology is complex, with both stimulatory and inhibitory effects of cell proliferation and with certain actions occurring independent of IGF-I (11–13, 47). The positive or negative modulatory effects of IGFBPs on IGF action are additionally altered by secreted proteases, including PSA and cathepsins (48–50).

Reports of positive correlation between elevated serum IGF-I levels and increased prostate cancer risk (51), of dysregulated IGF-I expression promoting development of prostatic neoplasia in transgenic mice (52, 53), and of up-regulated IGFBP-5 expression potentiating AI development in tumor models (36) have raised

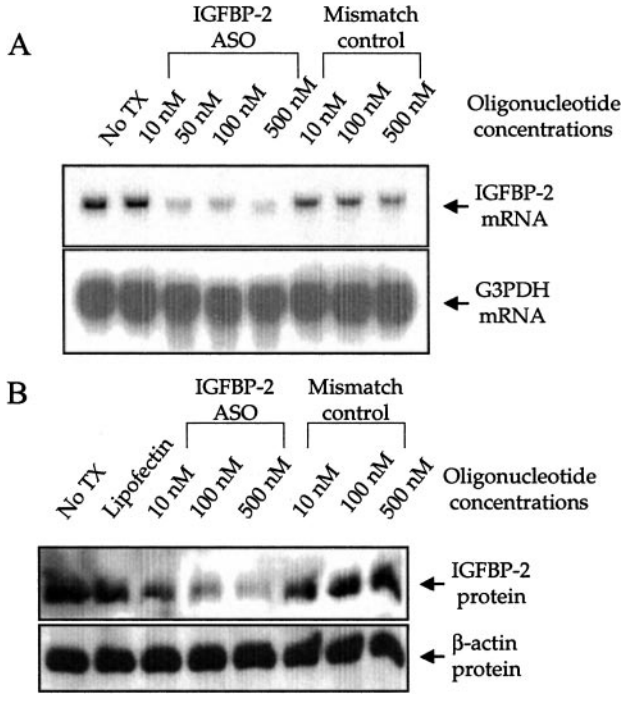

Fig. 6. Sequence-specific and dose-dependent suppression of IGFBP-2 mRNA and protein expression levels by IGFBP-2 ASO in LNCaP cells *in vitro*. *A*, LNCaP cells were treated with 10, 50, 100, and 500 nM IGFBP-2 ASO or mismatch control oligonucleotide for 4 days. Total cellular RNA was extracted and IGFBP-2 and G3PDH mRNA expression analyzed by Northern blotting. *No TX*, untreated cells. *B*, LNCaP cells were treated with 10, 50, 100, and 500 nM IGFBP-2 ASO or mismatch control oligonucleotide for 5 days, protein was extracted from cultured cells, and IGFBP-2 and β-actin protein levels were analyzed by Western blotting. *No TX*, untreated cells.

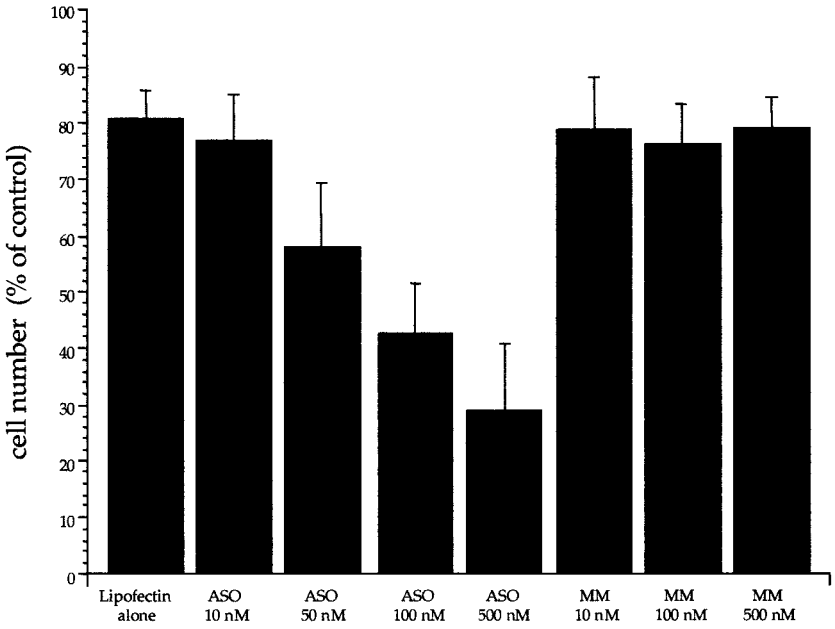

Fig. 7. Effects of IGFBP-2 ASO treatment on LNCaP cell growth *in vitro*. LNCaP cells were treated with IGFBP-2 ASO or mismatch control oligonucleotide in media containing 5% FCS. Cell number was determined using the crystal violet assay 3 days after treatment with IGFBP-2 ASO. Each point represents the mean of triplicate analysis with SD.

considerable interest in the role of the IGF axis in prostate carcinogenesis and progression. Of the various components of the IGF axis, the most significant castration-induced changes occur in levels of various IGFBPs. Expression patterns of certain IGFBPs in normal prostate epithelial cells change after castration or treatment with antiandrogens (27, 30, 31). Similarly, changes in expression of various IGFBPs have also been reported in prostate cancer, with increases in IGFBP-2 and IGFBP-5 and decreases in IGFBP-3 from the benign to malignant state (28–31, 54). IGFBP-3 and IGFBP-4 have apoptosis-inducing effects on prostate cancer cells, presumably by binding and inhibiting IGF-I activation of IGF-IR signaling (12, 48). Because IGFBP-3 antagonizes IGF-I signaling and IGFBP-2 and IGFBP-5 are thought to promote IGF responsiveness, castration-induced changes in IGFBP levels are consistent with a loss of IGF responsiveness in prostate cells undergoing androgen withdrawal-induced apoptosis and suggest that the ability to maintain IGF responsiveness through adaptive changes in IGFBP levels may be a key mechanism for survival of prostatic epithelial cells. We previously reported increasing IGFBP-5 levels in AD Shionogi tumors after castration and that IGFBP-5 ASOs inhibited IGF-I responsiveness and delayed AI progression postcastration (55). Forced overexpression of IGFBP-5 in LNCaP cells potentiated the antiapoptotic effects of IGF-I both *in vitro* and *in vivo* (36).

Increases in IGFBP-2 are associated with prostate cancer progression. IGFBP-2 immunohistochemical staining is higher in malignant compared with benign prostatic epithelial cells (30, 25). Elevated serum levels of IGFBP-2 have been positively correlated with the tumor stage of the patients and are assumed to originate from tumor cells (24). Bubendorf *et al.* (26) reported high IGFBP-2 expression in 100% of AI tumors, 36% of primary tumors, and 0% of benign prostate tissue in their human prostate cancer analysis by microarrays, suggesting a link between IGFBP-2 and AI progression.

In this study, we set out to characterize changes of IGFBP-2

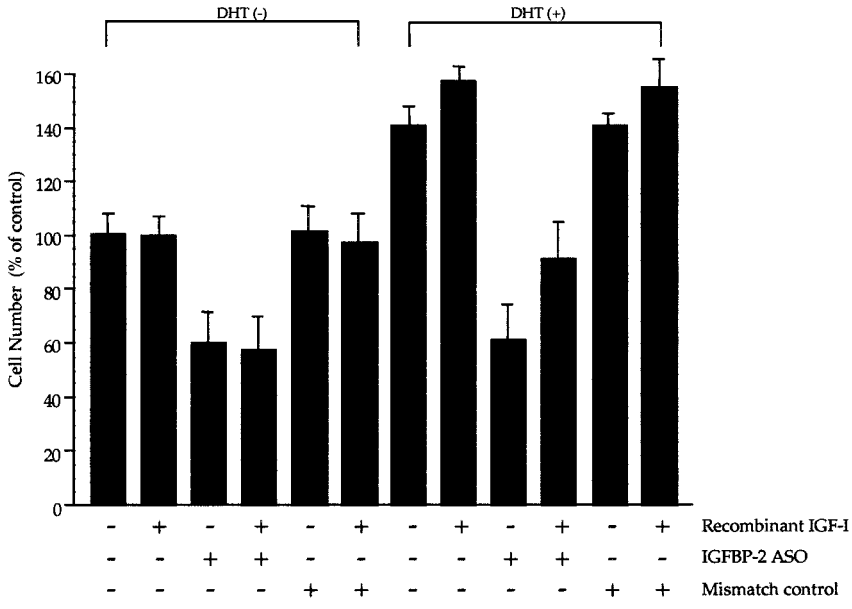

Fig. 8. Effects of DHT and IGF-I on IGFBP-2 ASO-induced LNCaP cell growth inhibition. After 24 h of serum starvation, LNCaP cells were treated with 500 nM IGFBP-2 ASO or mismatch control oligonucleotide for 2 days in the presence or absence of 1 nM DHT. Cells were stimulated with 100 ng/ml recombinant IGF-I 24 h after oligonucleotide treatment, and mitogenic assay was performed 24 h later to determine cell viability. Compared with untreated or mismatch control treated cells, IGFBP-2 ASO reduced LNCaP cell number by 56% with DHT and 40% without DHT, respectively. *, **, significantly different from untreated or mismatch control treated cells ($P < 0.05$). Each point represents the mean of triplicate analysis with SD.

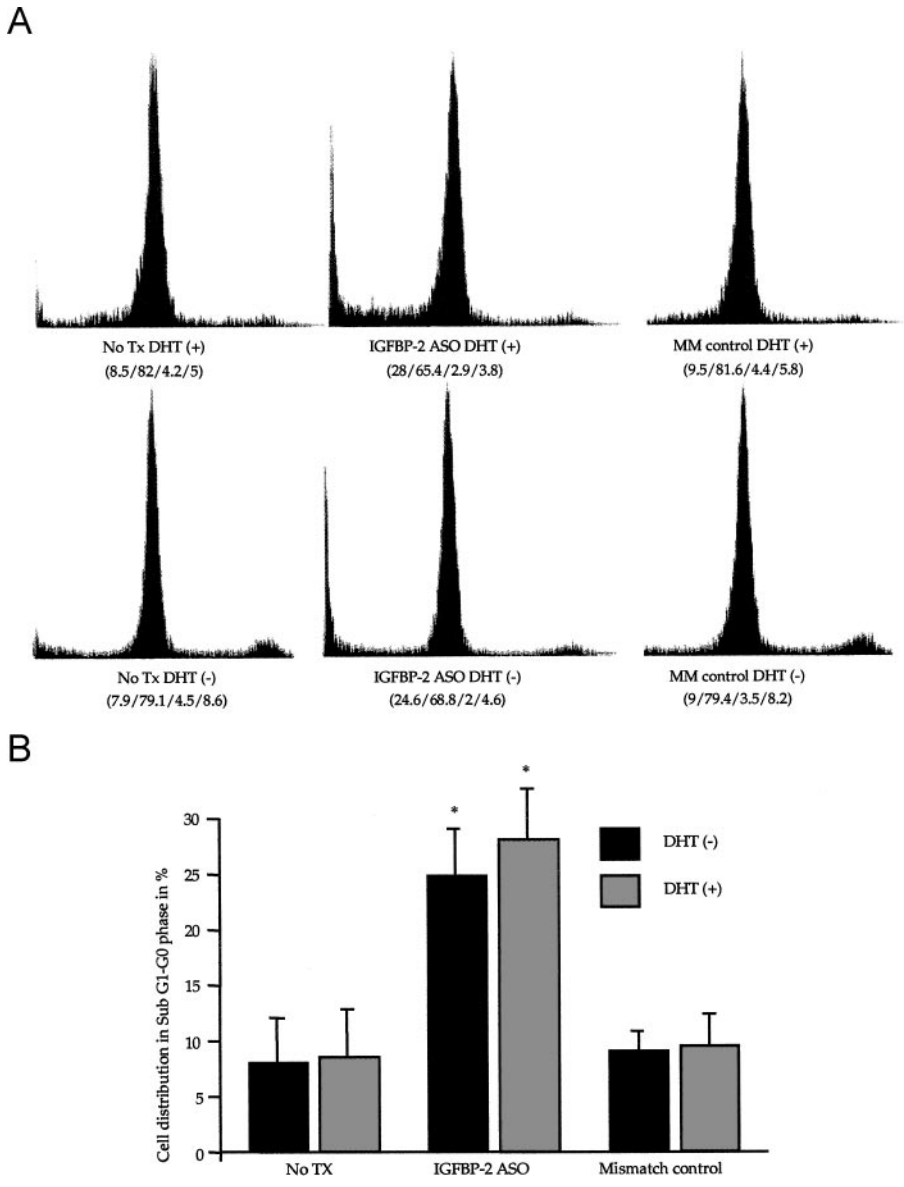

Fig. 9. LNCaP cell cycle analysis by flow cytometry after treatment with IGFBP-2 ASO. LNCaP cells were treated daily with IGFBP-2 ASO or mismatch control oligonucleotide with or without 1 nM DHT for 2 days. Cell population in each phase are shown in order of sub-G_1-G_0, G_1-G_0, S, and G_2 + M in percentages. Each data represents the mean value of triplicate experiments. After IGFBP-2 ASO treatment, the percentage of cells in sub-G_1-G_0 increased 3-fold ($P < 0.05$), whereas percentage of cells in G_2 + M decreased by 50%.

expression after androgen withdrawal and during AI progression and to assess the functional relevance of these changes using overexpression and antisense inhibition approaches in the LNCaP tumor model. The LNCaP tumor model is an androgen-sensitive, PSA-secreting human prostate cancer cell line that can be induced to form tumors in athymic mice under a variety of conditions. As in human prostate cancer, serum PSA levels in this model are regulated by androgen and are directly proportional to tumor volume. After castration, serum and tumor cell PSA levels decrease up to 80% and remain suppressed for 3–4 weeks. Beginning 4 weeks after castration, however, PSA production gradually increases above precastration levels in the absence of testicular androgens, heralding the onset of AI progression (43, 44). IGFBP-2 levels increased after androgen withdrawal *in vitro* and in AI tumors *in vivo* compared with AD tumors before castration, consistent with the human prostate cancer microarray analysis by Bubendorf *et al.* (26). Increases in IGFBP2 from benign to cancer and after androgen withdrawal of prostate cancers using tissue microarrays in this study support earlier reports and illustrate that increases in IGFBP-2 begin within months of androgen withdrawal. Increased IGFBP-2 levels after androgen withdrawal appear to play a functional role in progression because mean serum PSA and tumor volume increased more rapidly after castration in LNBP-2 transfectants and were delayed when IGFBP-2 levels were reduced by ASO treatment. Collectively, these findings link rising IGFBP-2 levels with the hormone refractory phenotype and indicate that inhibition of IGFBP-2 up-regulation after androgen withdrawal can delay AI growth.

These results confirm that targeting cell survival or mitogenic genes up-regulated after androgen withdrawal offers one strategy to delay tumor progression. ASO inhibit expression of target genes and can assess the functional relevance of candidate targets *in vivo*. The main advantage of ASO therapy is the capacity for systemic delivery and endocytic uptake into target cells, without the need for creation of special and complex delivery vectors. This is especially relevant when studying processes leading to AI progression, which cannot be reproduced in monolayer tissue cultures and must be studied in a limited number of animal tumor model systems. Phosphorothioate oligonucleotides are chemically stabilized to resist nuclease digestion and hybridize with target mRNA with high affinity. The specificity and efficacy of ASOs rely on precise targeting afforded by strand hybridization, which activates

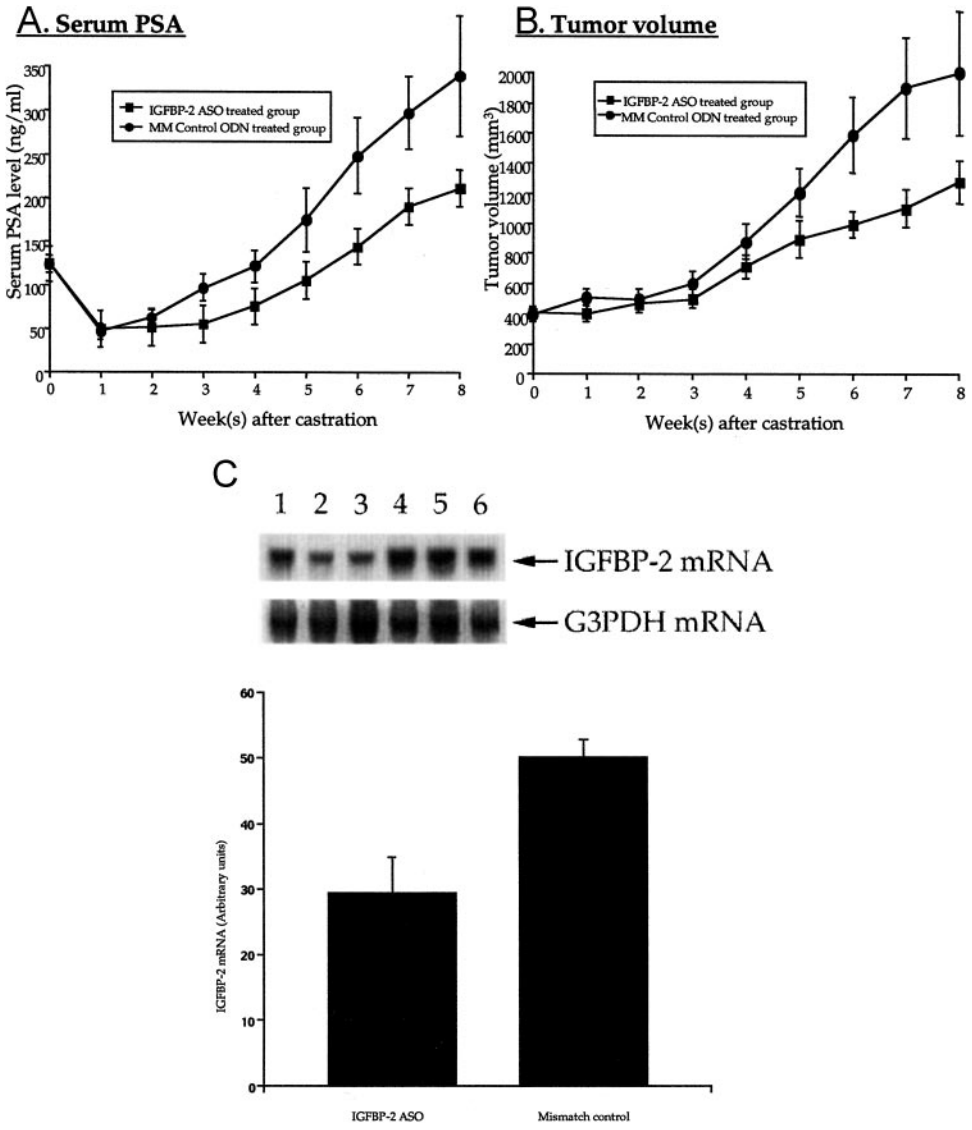

Fig. 10. Effect of IGFBP-2 ASO treatment on LNCaP tumor growth *in vivo*. LNCaP cells were inoculated s.c. into male athymic nude mice and mice bearing LNCaP tumors between 300 and 500 mm^3 in volume were castrated and treated with antisense or mismatch oligonucleotides by i.p. injection once daily. *A*, blood samples were obtained from the tail vain of the mice once weekly to measure serum PSA. By 8 weeks after castration, mean serum PSA level in IGFBP-2 ASO-treated mice was significantly lower than mismatch control ($P < 0.005$). *B*, tumor volume was measured once weekly and calculated by the formula: length $\times$ width $\times$ depth $\times$ 0.5236. By 8 weeks after castration, mean tumor volume in MM control-treated group was 1.6-fold higher than the IGFBP-2 ASO-treated group ($P < 0.05$). Each data point represents the mean tumor volume in each experimental group containing 7 mice with SD. Each point represents the mean of serum PSA levels in each experimental group containing 7 mice with SD. *C*, effects of IGFBP-2 ASO administration on IGFBP-2 mRNA levels in LNCaP tumors *in vivo* was assessed using Northern blotting from 3 IGFBP-2 ASO-treated (*Lanes 1–3*) and 3 MM oligonucleotide-treated (*Lanes 4–6*) tumors. IGFBP-2 mRNA levels were normalized to G3PDH mRNA levels, averaged for each treatment group, and expressed $\pm$ SD in the histogram. $*$, significantly different from mismatch-treated mice ($P < 0.05$).

RNaseH and prevents translation (56). Use of a 2-base mismatch oligonucleotide helps control for nonspecific immunomodulatory effects with phosphorothioate backbones.

In this study, an ASO targeted against IGFBP-2 translation initiation site was identified that potently suppressed IGFBP-2 mRNA and protein expression *in vitro* and *in vivo* in a dose-dependent and sequence-specific manner. In the *in vivo* experiments, mean serum PSA levels and tumor volume in mice bearing LNCaP tumors were significantly lower in mice treated with IGFBP-2 ASO compared with the mismatch control-treated group. These findings illustrate that *in vivo* systemic administration of an IGFBP-2 ASO can result in sequence specific down-regulation of the target gene in tumor tissues with delayed time to AI progression.

In vitro, ASO-induced decreases in IGFBP-2 inhibited serum-mediated LNCaP cell growth, both in the presence and absence of DHT. Flow cytometry analysis indicated that reduced cell numbers after IGFBP-2 ASO treatment resulted mainly from increased apoptosis either in the presence or absence of DHT. Although IGFBP-2 ASO decreased cell number to a greater degree in the presence of DHT, baseline absolute reduction in cell number was similar regardless of presence or absence of DHT. Fig. 8 indicates that IGF-I increases LNCaP cell proliferation and can partially overcome IGFBP-2 ASO growth inhibition only in the presence of DHT; indeed, IGF-I is not mitogenic and does not compensate for IGFBP-2 ASO inhibition in the absence of DHT. In the presence of DHT, IGF-I incompletely compensates for IGFBP-2 ASO inhibition of cell growth. These observations suggest that IGFBP-2 expression is necessary for efficient IGF-I-mediated cell growth by positively influencing the balance between apoptosis and proliferation.

LNCaP cells express trace levels of IGF-I mRNA, low levels of IGF-IR and no IRS-1 (45, 46) or trace amounts of IGFBP-5 (55). We (55) and others (57) have previously shown that IGF-I induces proliferation of LNCaP cells only in the presence of androgens. Furthermore, androgen ablation causes decreased IGF-IR mRNA levels in human LAPC-9 prostate cancer xenografts (54) and rat prostates (58). Taken together, these observations support a model in which androgen ablation results in reduced IGF-I responsiveness through reduced DHT and IGF receptor levels. The ability of the IGFBP-2 ASO treatment to significantly reduce LNCaP cell growth in both the presence and absence of IGF-I and under conditions in which LNCaP cells are both responsive (+DHT) and nonresponsive (−DHT) to IGF-I suggests that there may also be an IGF-I-independent pathway for IGFBP-2 to facilitate cell proliferation.

In summary, the results of this study support the hypothesis that increased IGFBP-2 expression after androgen ablation is an adaptive response that potentiates IGF-I-mediated cell survival and mitogene-

sis, thereby promoting AI tumor growth. Inhibiting IGFBP-2 expression using ASO technology may offer a treatment strategy to delay progression of prostate cancer after androgen withdrawal.

ACKNOWLEDGMENTS

We thank Eliana Beraldi, Mary Bowden, and Howard Tearle for their excellent technical assistance, as well as Dr. Lawrence Meyer and Visia Dragowska (Department of Molecular Sciences, British Columbia Cancer Agency, Vancouver, British Columbia, Canada) for their support and technical assistance in flow cytometry.

REFERENCES

1. Denis, L., and Murphy, G. P. Overview of Phase III trials on combined androgen treatment in patients with metastatic prostate cancer. Cancer (Phila.), *72:* 3888–3895, 1993.
2. Oh, W. K., and Kantoff, P. W. Management of hormone refractory prostate cancer: current standards and future prospects. J. Urol., *160:* 1220–1229, 1998.
3. Hudes, G., Einhorn, L., Ross, E., Balsham, A., Loehrer, P., Ramsey, H., Sprandio, J., Entmacher, M., Dugan, W., Ansari, R., Monaco, F., Hanna, M., and Roth, B. Phase II trial of 96-hour paclitaxel plus oral estramustine phosphate in metastatic hormone-refractory prostate cancer. J. Clin. Oncol., *15:* 3156–3163, 1997.
4. Petrylak, D. P., Macarthur, R. B., O'Connor, J., Shelton, G., Judge, T., Balog, J., Pfaff, C., Bagiella, E., Heitjan, D., Fine, R., Zuech, N., Sawczuk, I., Benson, M., and Olsson, C. A. Phase I trial of docetaxel with estramustine in androgen-independent prostate cancer. J. Clin. Oncol., *17:* 958–967, 1999.
5. Smith, D. C., Esper, D., Strawderman, M., Redman, B., and Pienta, K. J. Phase II trial of oral estramustine, oral etopside, and intravenous paclitaxel in hormone-refractory prostate cancer. J. Clin. Oncol., *17:* 1664–1671, 1999.
6. Macoulay, V. M. Insulin-like growth factors and cancer. Br. J. Cancer, *65:* 311–320, 1992.
7. Jones, J. I., and Clemmons, D. R. Insulin-like growth factor and their binding proteins: biological actions. Endocr. Rev., *16:* 3–34, 1995.
8. Ranke, M. B., and Elmlinger, M. Functional role of insulin-like growth factor binding proteins. Horm. Res., *48:* 9–15, 1997.
9. Zapf, J. Physiological role of the insulin-like growth factor binding proteins. Eur. J. Endocrinol., *132:* 645–654, 1995.
10. Shimasaki, S., and Ling, N. Identification and molecular characterization of insulin-like growth factor binding proteins (IGFBP-1, -2, -3, -4, -5, and -6). Prog. Growth Factor Res., *3:* 243–266, 1991.
11. LeRoith, D. Insulin-like growth factor. N. Engl. J. Med., *336:* 633–640, 1997.
12. Clemmons, D. R. Insulin-like growth factor binding protein and their role in controlling IGF actions. Cytokine Growth Factors Rev., *8:* 45–62, 1997.
13. Birnbaum, R. S., and Wiren, K. M. Changes in insulin-like growth factor binding protein expression and secretion during proliferation, differentiation, and mineralization of primary cultures of rat osteoblasts. Endocrinology, *135:* 223–230, 1994.
14. Cerro, J. A., Grewal, A., and Wood, T. L. Tissue-specific expression of the insulin-like growth factor binding protein (IGFBP) mRNAs in mouse and rat development. Regul. Pept., *48:* 189–198, 1993.
15. Green, B. N., Jones, S. B., Streck, R. D., Wood, T. L., Rotwein, P., and Pintar, J. E. Distinct expression patterns of insulin-like growth factor binding proteins 2 and 5 during fetal and postnatal development. Endocrinology, *134:* 954–962, 1994.
16. Cohen, P., Peehl, D. M., Lamson, G., and Rosenfeld, R. G. Insulin-like growth factors (IGFs), IGF receptors, and IGF-binding proteins in primary cultures of prostate epithelial cells. J. Clin. Endocrinol. Metab., *73:* 401–407, 1991.
17. Chen, J. C., Shao, Z. M., Sheikh, M. S., Hussain, A., Leroth, D., Roberts, C. T., and Fontana, J. A. Insulin-like growth factor-binding protein enhancement of insulin-like growth factor-I (IGF-I)-mediated DNA synthesis and IGF-I binding in a human breast carcinoma cell line. J. Cell. Physiol., *158:* 69–78, 1994.
18. Andreas, H., Olga, F., Harald, L., Werner, F. B., Helmut, J. K., Dieter, E., Eckhard, W., and Matthias, M. W. Overexpression of insulin-like growth factor-binding protein-2 results in increased tumorigenic potential in Y-1 adenocortical tumor cells. Cancer Res., *60:* 834–838, 2000.
19. Flybjerg, A., Mogensen, B., and Nielsen, O. S. Elevated serum insulin-like growth factor-binding protein 2 (IGFBP-2) and decreased IGFBP-3 in epithelial ovarian cancer: correlation with cancer antigen 125 and tumor-associated trypsin inhibitor. J. Clin. Endocrinol. Metab., *82:* 2308–2313, 1997.
20. El Atiq, F., Garrouste, F., Remacle-Bonnet, M., Sastre, B., and Pommier, G. Alterations in serum levels of insulin-like growth factors and insulin-like growth factor binding proteins in patients with colorectal cancer. Int. J. Cancer, *57:* 491–497, 1994.
21. Miller, H. L., Oh, Y., Lehenbecher, T., Blum, W. F., and Rosenfeld, R. G. Insulin-like growth factor-binding protein-2 concentrations in cerebrospinal fluid and serum of children with malignant solid tumors or acute leukemia. J. Clin. Endocrinol. Metab., *79:* 428–434, 1994.
22. Ho, P. J., and Baxter, R. C. Insulin-like growth factor-binding protein-2 in patients with prostate carcinoma and benign prostatic hyperplasia. Clin. Endocrinol., *46:* 333–342, 1997.
23. Kanety, H., Madjar, Y., Dagan, Y., Levi, J., Papa, M. Z., Pariente, C., Goldwasser, B., and Karasik, A. Serum insulin-like growth factor binding-protein-2 (IGFBP-2) is increased and IGFBP-3 is decreased in patients with prostate cancer: correlation with serum prostate-specific antigen. J. Clin. Endocrinol. Metab., *77:* 229–233, 1993.
24. Cohen, P., Peehl, D. M., Stamey, T. A., Wilson, K. F., Clemmons, D. R., and Rosenfeld, R. G. Elevated levels of insulin-like growth factor-binding protein-2 in the serum of prostate cancer patients. J. Clin. Endocrinol. Metab., *76:* 1031–1035, 1993.
25. Figueroa, J. A., DeRaad, S., Tadlock, L., Speights, V. O., and Rinehart, J. J. Differential expression of insulin-like growth factor binding proteins in high *versus* low Gleason score prostate cancer. J. Urol., *159:* 1379–1383, 1998.
26. Bubendorf, L., Kolmer, M., Kononen, J., Koivisto, P., Mousses, S., Chen, Y., Mahlamaki, E., Schraml, P., Moch, H., Willi, N., Elkahloun, A. G., Pretlow, T. G., Gasser, T. C., Mihatsch, M. J., Sauter, G., and Kallioniemi, O. P. Hormone therapy failure in human prostate cancer: analysis by complementary DNA and tissue microarrays. J. Natl. Cancer Inst. (Bethesda), *91:* 1758–1764, 1999.
27. Thomas, L. N., Wright, A. S., Lazier, C. B., Cohen, P., and Rittmaster, R. Prostatic involution in men taking finasteride is associated with elevated levels of insulin-like growth factor-binding proteins (IGFBPs)-2, -4, and -5. Prostate, *42:* 203–210, 2000.
28. Nickerson, T., Miyake, H., Gleave, M. E., and Pollak, M. Castration-induced apoptosis of androgen-dependent Shionogi carcinoma is associated with increased expression of genes encoding insulin-like growth factor-binding proteins. Cancer Res., *59:* 3392–3395, 1999.
29. Naggabhushan, M., Miller, C. M., Pretlow, T. P., Giaconia, J. M., Edgehouse, N., Schwartz, S., Kung, H. J., de Vere White, R. W., Gumerlock, P. H., Resnick, M. I., Amini, S. B., and Pretlow, T. G. CWR22: the first human prostate cancer xenograft with strongly androgen-dependent and relapsed strains both *in vivo* and in soft agar. Cancer Res., *56:* 3042–3046, 1996.
30. Tennant, M. K., Thrasher, J. B., Twomey, P. A., Birnbaum, R. S., and Plymate, S. R. Insulin-like growth factor-binding protein-2 and -3 expression in benign human prostate epithelium, prostate intraepithelial neoplasia, and adenocarcinoma of the prostate. J. Clin. Endocrinol. Metab., *81:* 411–420, 1996.
31. Thrasher, J. B., Tennant, M. K., Twomey, P. A., Hansberry, K. L., Wettlauer, J. N., and Plymate, S. R. Immunohistochemical localization of insulin-like growth factor binding proteins 2 and 3 in prostate tissue: clinical correlations. J. Urol., *155:* 999–1003, 1996.
32. Memouny, N., Binoux, M., and Babajko, S. IGFBP-2 expression in a human line is associated with increased IGFBP-3 proteolysis, decreased IGFBP-1 expression and increased tumorigenicity. Int. J. Cancer, *77:* 874–879, 1998.
33. Gleave, M., Tolcher, A., Miyake, H., Nelson, C., Brown, B., Beraldi, E., and Goldie, J. Progression to androgen independence is delayed by adjuvant treatment with antisense bcl-2 oligodeoxynucleotides after castration in the LNCaP prostate tumor model. Clin. Cancer Res., *5:* 2891–2898, 1999.
34. Miyake, H., Monia, B. P., and Gleave, M. E. Inhibition of progression to androgen-independence by combined adjuvant treatment with antisense Bcl-xL and antisense Bcl-2 oligonucleotides plus Taxol after castration in the Shionogi tumor model. Int. J. Cancer, *86:* 855–862, 2000.
35. Miyake, H., Nelson, C., Rennie, P. S., and Gleave, M. E. Testosterone-repressed prostate message-2 is an antiapoptotic gene involved in progression to androgen independence in prostate cancer. Cancer Res., *60:* 170–176, 2000.
36. Miyake, H., Nelson, C., Rennie, P. S., and Gleave, M. E. Overexpression of insulin-like growth factor binding protein-5 helps accelerate progression to androgen-independence in the human prostate LNCaP tumor model through activation of phosphatidylinositol 3′-kinase pathway. Endocrinology, *141:* 2257–2265, 2000.
37. Chi, K., Gleave, M., Klasa, R., Bryce, C., Murray, N., D'Aloisio, S., Lopes de Menezes, D., and Tolcher, A. A Phase I dose finding study of combined treatment with an antisense Bcl-2 oligonucleotide (Genasense) and mitoxantrone in patients with metastatic androgen-independent prostate cancer. Clin. Cancer Res., *7:* 3920–3927, 2001.
38. Zellweger, T., Miyake, H., Monia, B., Cooper, S., and Gleave, M. Efficacy of antisense clusterin oligonucleotides is improved *in vitro* and *in vivo* by incorporation of 2′-o-(2-methoxy) ethyl chemistry. J. Pharmacol. Exp. Ther., *298:* 934–940, 2001.
39. Monia, B. P., Johnston, J. F., Geiger, T., Muller, M., and Fabbro, D. Antitumor activity of a phosphorothioate antisense oligodeoxynucleotide targeted against C-raf kinase. Nat. Med., *2:* 668–675, 1996.
40. Cucco, C., and Calabretta, B. In vitro and in vivo reversal of multidrug resistance in a human leukemia-resistant cell line by mdr1 antisense oligodeoxynucleotides. Cancer Res., *56:* 4332–4337, 1996.
41. Ziegler, A., Luedke, G. H., Fabbro, D., Altmann, K. H., Stahel, R. A., and Zangemeister-Wittke, U. Induction of apoptosis in small-cell lung cancer cells by an antisense oligodeoxynucleotide targeting the Bcl-2 coding sequence. J. Natl. Cancer Inst. (Bethesda), *89:* 1027–1036, 1997.
42. Jansen, B., Schlagbauer-Wadl, H., Brown, B. D., Bryan, R. N., van Elsas, A., Muller, M., Wolff, K., Eichler, H. G., and Pehamberger, H. bcl-2 antisense therapy chemosensitizes human melanoma in SCID mice. Nat. Med., *4:* 232–234, 1998.
43. Gleave, M., Hsieh, J. T., Wu, H. C., von Eschenbach, A. C., and Chung, L. W. Serum prostate-specific antigen levels in mice bearing human prostate LNCaP tumors are determined by tumor volume and endocrine and growth factors. Cancer Res., *52:* 1598–1605, 1992.
44. Gleave, M. E., Hsieh, J. T., Gao, C., von Eschenbach, A. C., and Chung, L. W. K. Acceleration of human prostate carcinoma growth *in vivo* by factors produced by prostate and bone fibroblasts. Cancer Res., *51:* 3753–3761, 1991.
45. Yu, D., Chen, D., Chiu, C., Razmazma, B., Chow, Y. H., and Pang, S. Prostate-specific targeting using PSA promoter-based lentiviral vectors. Cancer Gene Ther. *8:* 628–635, 2001.
46. Craft, N., Shostak, Y., Carey, M., and Sawyers, C. L. A mechanism for hormone-independent prostate cancer through modulation of androgen receptor signaling by the HER-2/neu tyrosine kinase. Nat. Med., *5:* 280–285.
47. Miyakoshi, N., Ricman, C., Kasukawa, Y., Linkhart, T. A., Baylink, D. J., and Mohan, S. Evidence that IGF-binding protein functions as a growth factor. J. Clin. Investig., *107:* 73–81, 2001.

48. Cohen, P., Peehl, D. M., and Rosenfeld, R. G. The IGF axis in the prostate. Horm. Metab. Res., *26:* 81–84, 1994.
49. Conover, C. A., Perry, J. E., and Tindall, D. J. Endogenous cathepsin D-mediated hydrolysis of insulin-like growth factor-binding proteins in cultured human prostatic carcinoma cells. J. Clin. Endocrinol. Met., *80:* 987–993, 1995.
50. Manes, S., Llorente, M., Lacalle, R. A., Gomez-Mouton, C., Kremer, L., Mira, E., and Martinez, A. The matrix metalloproteinase-9 regulates the insulin-like growth factor-triggered autocrine response in DU-145 carcinoma cells. J. Biol. Chem., *274:* 6935–6945, 1999.
51. Chan, J. M., Stampfer, M. J., Giovannucci, Gann, P. H., Ma, J., Wilkinson, P., Hennekens, C. H., and Pollak, M. Plasma insulin-like growth factor I and prostate cancer risk: a prospective study. Science (Wash. DC), *279:* 563–566, 1998.
52. DiGiovanni, J., Kiguchi, K., Frijhoff, A., Wilker, E., Bol, D. K., Beltran, L., Moats, S., Ramirez, A., Jorcano, J., and Conti, C. Deregulated expression of insulin-like growth factor I in prostate epithelium leads to neoplasia in transgenic mice. Proc. Natl. Acad. Sci. USA, *97:* 3455–3460, 2000.
53. Kaplan, P. J., Mohan, S., Cohen, P., Foster, B. A., and Greenberg, N. M. The insulin-like growth factor axis and prostate cancer: lessons from the transgenic adenocarcinoma of mouse prostate (TRAMP) model. Cancer Res., *59:* 2203–2209, 1999.
54. Nickerson, T., Chang, F., Lorimer, D., Smeakins, S. P., Sawyers, C. L., and Pollak, M. *In vivo* progression of LAPC-9 and LNCaP prostate cancer models to androgen independence is associated with increased expression of insulin-like growth factor I (IGF-I) and IGF-I receptor (IGF-IR). Cancer Res., *61:* 6276–6280, 2001.
55. Miyake, H., Pollak, M., and Gleave, M. E. Castration-induced up-regulation of insulin-like growth factor binding protein-5 potentiates insulin-like growth factor-I activity and accelerates progression to androgen independence in prostate cancer models. Cancer Res., *60:* 3058–3064, 2000.
56. Crooke, S. T. Molecular mechanisms of antisense drugs: RNase H. Antisense Nucleic Acid Drug Dev., *8:* 133–134, 1998.
57. Iwamura, M., Sluss, P. M., Casamento, J. B., and Cockett, A. T. Insulin-like growth factor I: action and receptor characterization in human prostate cancer cell lines. Prostate, *22:* 243–252, 1993.
58. Huynh, H., Seyam, R. M., and Brock, G. M. Reduction of ventral prostate weight by finasteride is associated with suppression of insulin-like growth factor I (IGF-I) and IGF-I receptor genes and with an increase in IGF binding protein 3. Cancer Res., *58:* 215–218, 1998.